The Astrophysical Journal, 654: L163–L166, 2007 January 10

A SEMIEMPIRICAL MAGNETOHYDRODYNAMICAL MODEL OF THE SOLAR WIND

O. Cohen,[1] I. V. Sokolov,[1] I. I. Roussev,[2] C. N. Arge,[3] W. B. Manchester,[1] T. I. Gombosi,[1]
R. A. Frazin,[4] H. Park,[4] M. D. Butala,[4] F. Kamalabadi,[4] and M. Velli[5]
Received 2006 October 17; accepted 2006 November 27; published 2006 December 21

ABSTRACT

We present a new MHD model for simulating the large-scale structure of the solar corona and solar wind under "steady state" conditions stemming from the Wang-Sheeley-Arge empirical model. The processes of turbulent heating in the solar wind are parameterized using a phenomenological, thermodynamical model with a varied polytropic index. We employ the Bernoulli integral to bridge the asymptotic solar wind speed with the assumed distribution of the polytropic index on the solar surface. We successfully reproduce the mass flux from Sun to Earth, the temperature structure, and the large-scale structure of the magnetic field. We reproduce the solar wind speed bimodal structure in the inner heliosphere. However, the solar wind speed is in a quantitative agreement with observations at 1 AU for solar maximum conditions only. The magnetic field comparison demonstrates that the input magnetogram needs to be multiplied by a scaling factor in order to obtain the correct magnitude at 1 AU.

Subject headings: interplanetary medium — methods: numerical — MHD — solar wind — Sun: evolution — Sun: magnetic fields

1. INTRODUCTION

The solar wind origin, acceleration, and heating have been debated by the solar-heliospheric community for decades. Although there is significant progress in this area, the available theoretical models for turbulent processes in the solar wind (i.e., turbulent heating) cannot provide yet a reliable and quantitatively accurate agreement with the observed solar wind parameters at 1 AU. We also lack a detailed description of the three-dimensional structure of the interplanetary magnetic field, which affects the transport of solar energetic particles through the heliosphere.

The theory of solar wind origin and evolution is challenged by the following two fundamental problems. In the first place stands the "coronal heating" problem; the temperature in the solar atmosphere rises by 2 orders of magnitude from the photosphere ($T < 10^4$ K) to the corona ($T_e \approx T_i \approx 10^6$ K) across a narrow transition region (Aschwanden 2004). The coronal plasma expands into the interplanetary space, guided by the magnetic field close to the Sun, to form the solar wind. Second, there is a discrepancy between the observed values of coronal temperature and the observed solar wind speeds in the inner heliosphere (IH), in particular at 1 AU. The solar wind at a heliocentric distance of 1 AU has a speed of $u_{sw} \sim 800$ km s^{-1} when originating from regions of open magnetic field lines; this is the so-called fast solar wind. On the other hand, the solar wind associated with regions of closed field lines (or helmet streamers) is slow, with a speed of $u_{sw} \sim 400$ km s^{-1}; this is the so-called slow solar wind. In both cases, the kinetic energy of a pair of proton and electron is much greater than their thermal energy in the solar corona (SC): $m_p(400 \text{ km s}^{-1})^2/2k_B \approx 10^7 \text{ K} \gg 2T = T_e + T_i$. The discrepancy for the fast solar wind is more than an order of magnitude. Note that even the gravitational potential energy at the solar surface is greater than the coronal temperature: $GM_\odot m_p/R_\odot k_B = 2.3 \times 10^7 \text{ K} \gg 2T$. Therefore, the theory needs to explain how the solar wind plasma originates from the Sun, how it is accelerated to escape the solar gravity, and how it is further powered to reach the observed speed and the bimodal structure in the IH.

Numerical reproduction of the SC steady state conditions has been extensively investigated since the famous work by Pneuman & Kopp (1971). Traditionally, the deposition of energy and/or momentum into the solar wind has been described by means of some empirical source terms (Usmanov 1993; McKenzie et al. 1997; Mikić et al. 1999; Suess et al. 1999; Wu et al. 1999; Groth et al. 2000, e.g.). In these models, the sources of plasma heating and solar wind acceleration are typically modeled in a qualitative sense, and the spatial profiles for the deposition of the energy or momentum are usually modeled by exponentials in radial distance. In more realistic models, the solar wind is heated and accelerated by the energy and momentum interchange between the solar plasma and large-scale Alfvén turbulence (Jacques 1977; Dewar 1970; Barnes 1992; Usmanov et al. 2000; Usmanov & Goldstein 2003).

Due to the insufficient comparison with observations at 1 AU, it is reasonable to adopt semiempirical models. Assimilating a long history of solar wind observations, these models are very efficient and accurate. A particular example is the Wang-Sheeley-Arge (WSA) model (Arge & Pizzo 2000; Arge et al. 2003, 2004). This model uses the observed photospheric magnetic field to determine the coronal field configuration, which is then used to estimate the distribution of the final speed of the solar wind, u_{sw}. The common disadvantage of semiempirical models is that they are physically incomplete.

Here we present an improved three-dimensional MHD model for the steady state solar wind in the SC and IH. The WSA model is used as an input for a three-dimensional MHD code, in which the processes of turbulent heating in the solar wind are parameterized using a phenomenological, thermodynamical model with a varied polytropic index. The application of varied polytropic index had been described in Roussev et al. (2003). We employ the Bernoulli integral to bridge the observed solar

[1] Department of Atmospheric, Oceanic, and Space Sciences, University of Michigan, Ann Arbor, MI; oferc@umich.edu.
[2] Institute for Astronomy, Honolulu, HI; iroussev@ifa.hawaii.edu.
[3] Air Force Research Laboratory/Space Vehicles Directorate, Hanscom Air Force Base, MA; nick.arge@hanscom.af.mil.
[4] Department of Electrical and Computer Engineering, University of Illinois, Urbana, IL; frazin@uiuc.edu.
[5] Jet Propulsion Laboratory, California Institute of Technology, Pasadena, CA; mvelli@jpl.nasa.gov.

wind speed at 1 AU with the assumed distribution of the polytropic index on the solar surface. We describe the model in § 2 and the simulation setup in § 3. We present and discuss the simulation results in § 4.

2. SEMIEMPIRICAL SOLAR WIND MODEL

The WSA model, an improved version of the original model by Wang & Sheeley (1990), derives the final solar wind speed from magnetogram data. It employs a potential magnetic field extrapolation (Altschuler & Newkirk 1969; Altschuler et al. 1977) for the SC. After the magnetic field distribution is calculated in between the solar surface and the source surface (usually set at $R_{ss} = 2.5\,R_\odot$), the model generates an expansion factor, f_s, for the magnetic flux tube defined as $f_s = (R_\odot/R_{ss})^2[B(R_\odot)/B_0(R_{ss})]$. Here B is the field strength. Using solar wind data, the model relates the final solar wind speed to the expansion factor. An improved relationship also takes into account the minimum angular distance of open flux tubes from the boundary of coronal holes, θ_b, and reads

$$u_{sw} = 265 + \frac{25}{f_s^{2/7}}(5.0 - 1.1e^{1-(\theta_b/4)^2})^2 \text{ km s}^{-1}. \quad (1)$$

A way to incorporate this empirical relationship to our MHD model—including neither the potential field expansion nor the potential field at all—is to relate the solar wind speed to the spatial distribution of the Bernoulli integral throughout the SC and IH (Parker 1963; Fisk 2003; Suzuki 2006). Let us assume that the model for the SC and IH fulfills the Bernoulli integral. Then, at each point, $\boldsymbol{R}$, the solar wind kinetic energy can be obtained using the Bernoulli equation, with the pressure function being an integral from an infinitely distant point to $\boldsymbol{R}$ along a solar wind streamline:

$$\int_0^{p(R)} \frac{dp}{\rho} + \frac{u^2(R)}{2} - \frac{GM_\odot}{R} = \frac{u_{sw}^2}{2}. \quad (2)$$

Here u_{sw} is the final solar wind speed given by equation (1). The integral term is the work done in the course of plasma expansion from pressure $p(R)$ to vacuum ($p = 0$). This work is equal to the gain in total energy (kinetic plus potential), so that equation (2) represents the energy conservation along a streamline. For an adiabatic expansion ($ds = 0$), $dp/\rho = dw - T\,ds/\rho = d(\epsilon + p/\rho)$. Since the internal energy, ϵ, is $(p/\rho)/(\gamma - 1)$, one can get the pressure function for a polytropic gas:

$$\int_0^{p(R)} \frac{dp}{\rho} = \int_0^{p(R)} d\left(\frac{\gamma}{\gamma - 1}\frac{p}{\rho}\right) = \frac{\gamma(R)}{\gamma(R) - 1}\frac{p(R)}{\rho(R)}. \quad (3)$$

Equation (3) enables one to relate the Bernoulli integral to the polytropic index through the boundary values at the Sun:

$$\frac{\gamma p}{(\gamma - 1)\rho}\Big|_{R_\odot} = \frac{u_{sw}^2}{2} + \frac{GM_\odot}{R}. \quad (4)$$

Thus, by tracing the magnetic field lines down to the photosphere and, assuming that the surface speed is zero and that the gravity is known, we can obtain the distribution of γ on the solar surface in terms of the coronal base temperature $T_\odot = p/\rho|_{R_\odot}$ and the solar wind speed u_{sw} originating from this point, which is given by equation (1).

Our approach adopts the Bernoulli integral, which is alternative to the widely used volumetric heating functions. The disadvantage of the latter is that one needs to guess the unknown three-dimensional distribution of the heat sources and to compare with the observed solar wind speed, which is some nonlinear function of these heating sources. The Bernoulli integral, on the other hand, depends only on the distribution of the solar wind parameters extracted from the WSA model. Therefore, this approach should result in a more realistic solution.

3. SIMULATION

We apply the model to the SC module of the Space Weather Modeling Framework code in a similar manner as described in (Tóth et al. 2005). We choose to simulate the steady state SC during solar minimum conditions (Carrington rotation [CR] 1922) and solar maximum conditions (CR 1958). The initial grid refinement is of nine levels, with smallest grid size of $1/42\,R_\odot$ on the solar surface and largest grid size of $3/4\,R_\odot$.

We calculate the potential field using harmonic coefficients obtained by the Wilcox Solar Observatory[6] and extract from it the initial distribution of the magnetic field for the domain $R_\odot \le r \le R_{ss}$ ($R_{ss} = 2.5\,R_\odot$). Once the potential field is obtained, we can calculate all the input parameters for the WSA model. The polytropic index distribution in between $R_\odot < R < R_{ss}$ is calculated at the auxiliary spherical grid in a manner as follows. We trace the potential field line through each grid point and find the solar wind speed, u_{sw}, using equation (1) at the end of this field line. Using equation (4) and assuming the constant coronal base temperature $2T_0 = T_e + T_i = 2 \times 10^6$ K, we find the polytropic index value $\gamma(R_\odot)$ at the footpoint of the same field line. Depending on the heliocentric distance, R, of the auxiliary grid point, we interpolate the value of the polytropic index, γ, between the coronal base value $\gamma(R_\odot)$ and the constant value $\gamma_{ss} = 1.1$ at the source surface. Above the source surface in the MHD code, γ is linearly increased toward 1.5 between $R_{ss} \le R < 12.5\,R_\odot$, and $\gamma = 1.5$ above $R \ge 12.5\,R_\odot$.

Note that the Bernoulli-integral approach, which is valid for most of the spatial domain, does not hold true in the current sheet. Therefore, above the source surface, we impose the value of γ to approach 1.1 in the current sheet, where the plasma $\beta = nk_B T/(B^2/2\mu_0) > 1$. Since the polytropic index represents the level of turbulence of the plasma, we assume that in the current sheet the gas has some amount of turbulence. In addition, constraining γ in the current sheet to be the same as on the source surface ensures that the gradient of γ never points toward the Sun; therefore, there is no sunward acceleration.

After setting the above distribution of γ, we solve the MHD equations self-consistently. In order to obtain the correct solar wind solution, it is necessary to choose an appropriate inner boundary condition for the density (Hammer 1982; Suzuki & Inutsuka 2005). The boundary value for the density at the corona base (the base density), $\rho_b(\phi, \theta)$, is chosen to be anticorrelated with the solar wind speed, $u_{sw}(\phi, \theta)$, which originates from the surface point with the longitude, ϕ, and latitude, θ. Specifically, we apply the following boundary condition: $\rho_b(\phi, \theta) = [u_{min}/u_{sw}(\phi, \theta)]^2 \times 10^9$ cm^{-3}, where u_{min} is the minimum solar wind speed in the WSA model. As a result, the base density in the open field region is by a factor of 3 smaller than that in the closed field region.

4. RESULTS AND DISCUSSION

The left panel of Figure 1 shows the steady state results for the SC for CR 1922. Our model reproduces the bimodal solar wind with fast wind (650–850 km s^{-1}) at high latitudes and

[6] See http://sun.stanford.edu.

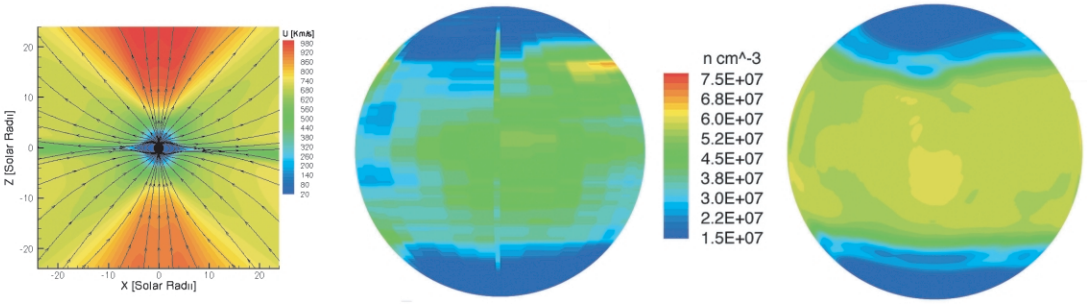

FIG. 1.—Simulation results for the solar corona for CR 1922 are shown in the left panel, where color contours represent speed and streamlines represent magnetic field lines. The middle and right panels show electron density isosurfaces for a height of $r = 1.3\ R_{\odot}$. The middle panel shows electron density extracted from tomographic Mauna Loa MkIII measurements, and the right panel shows the electron density calculated by the simulation.

slow wind (350–400 km s^{-1}) at low latitudes. The magnetic field lines are opened into the heliosphere by the fast solar wind, and a thin current sheet is formed along the surface of polarity reversal of the radial magnetic field. The middle and right panels of Figure 1 show a comparison of the simulation result for the electron density with the tomographic reconstruction of the Mauna Loa Mark III K-coronameter (MkIII) measurements (Frazin & Janzen 2002). The agreement is noticeable, except for a few small-scale features, which may be artifacts of the reconstruction.

Figure 2 shows the simulation results compared with *Advanced Composition Explorer* (*ACE*) observations at 1 AU for CR 1958. The modeled density follows the observations with discrepancies of less than a factor of 3 from the observed values. The temperature obtained from the simulation is of the same order as the observations. It can be seen that where the temperature is lower than the observed values, the density is higher, and vice versa. The kinetic gas pressure, however, is consistent with in situ observations at 1 AU. In order to reach the agreement with observations of the magnetic field intensity, we had to apply a scaling factor of 4 to the used magnetogram. It is unclear whether this discrepancy is (1) a shortcoming of the model, (2) due to uncertainties in the photospheric magnetic field measurements, or (3) a shortcoming of the potential field approximation. This issue of the "scaling factor," along with the reliability of the potential field approximation, is actively debated at conferences (e.g., SHINE 2006 workshop) but not in the literature. This remains to be investigated. Using this correction, the trends of the magnetic field predicted by the model match the observed field at 1 AU both in terms of structure and magnitude. The solar wind speed predicted by the simulation agrees with the observations as well as with the speed predicted by the WSA model. In addition to the parameters predicted by the WSA model—for example, the solar wind speed and the magnetic field polarity at a specific point—our model can predict all the physical parameters everywhere

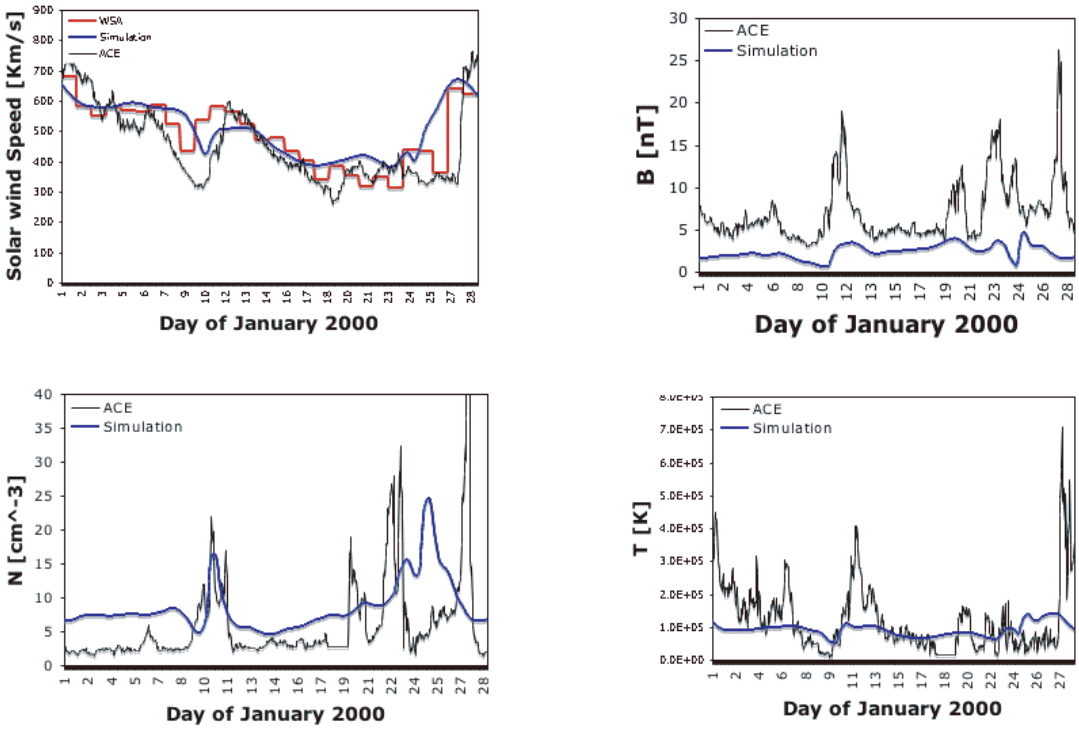

FIG. 2.—Comparison of the simulation results (*blue line*) with *ACE* data (*black line*) and the WSA model (*red line*; speed only) for CR 1958. Plots are shown for solar wind speed (*top left*), magnetic field (*top right*), number density (*bottom left*), and temperature (*bottom right*).

within the computation domain with good agreement with observations. The model predictions of the solar wind parameters at 1 AU for solar minimum conditions (CR 1922) are similar to the solar maximum case, except for the solar wind speed, which is approximately 100 km s^{-1} faster than that observed.

The choice of solar wind model in numerical investigations of processes in the SC, IH, and outer heliosphere is a matter of crucial importance for space weather. We developed a numerical implementation of empirical models to reproduce the ambient solar wind conditions. From the physical perspective, it is important to have the correct background conditions in order to simulate a space weather event. From the practical aspect, it is necessary to have a model with prescribed parameters, in order to approach an automation of space weather forecasting tools. Our model reproduces the ambient solar wind observations rather well and, in addition, it uses only magnetograms as input.

Our model succeeds in reproducing the mass flux from Sun to Earth. The density structure both at the SC and at 1 AU matches very well the observations. The simulated temperature agrees with observations as well. The magnetic field general structure is correct, with the open and closed field line regions in the SC and a thin current sheet between the north and south hemispheres. The bimodal solar wind speed is reproduced with fast wind at high latitudes and slow wind at low latitudes. However, the solar wind speed at 1 AU is found to be faster than that observed for solar minimum conditions. The studied solar-maximum case does not show such behavior, and the solar wind speed is correctly reproduced at 1 AU. The explanation for this discrepancy may be as follows. In deriving the coefficients in equation (1), the ballistic propagation of the solar wind with a constant speed is assumed from the source surface to 1 AU. This holds true neither in our model nor in reality, since the solar wind can be further accelerated beyond the source surface. In addition, it seems that for the particular case of solar minimum, it is harder to get the correct speed when comparing with observations because the location of the spacecraft relative to the current sheet can be easily missed (Arge et al. 2004).

We will continue to improve and validate the model as we investigate a series of Carrington rotations over the past and present solar cycles.

The authors would like to thank L. Svalgaard, A. Usmanov, P. Roe, and an unknown referee for their comments, and Yang Liu for providing the magnetogram data. The research for this manuscript is supported by Department of Defense MURI grant F49620-01-1-0359, ATM grant 03-18590, and NASA AISRP grant NAG5-9406 at the University of Michigan, and in part by NSF grant ATM 05-55561 at the University of Illinois. I. I. R. has been partially supported by NSF SHINE grant ATM-0631790. I. V. S. is supported by contract F014254 between the Jet Propulsion Laboratory and the University of Michigan.

REFERENCES

Altschuler, M. D., Levine, R. H., Stix, M., & Harvey, J. 1977, Sol. Phys., 51, 345
Altschuler, M. D., & Newkirk, G. 1969, Sol. Phys., 9, 131
Arge, C. N., Luhmann, J. G., Odstrcil, D., Schrijver, C. J., & Li, Y. 2004, J. Atmos. Terr. Phys., 66, 1295
Arge, C. N., Odstrcil, D., Pizzo, V. J., & Mayer, L. R. 2003, in AIP Conf. Proc. 679, Solar Wind Ten, ed. M. Velli, R. Bruno, & F. Malara (New York: AIP), 190
Arge, C. N., & Pizzo, V. J. 2000, J. Geophys. Res., 105, 10,465
Aschwanden, M. J. 2004, Physics of the Solar Corona: An Introduction (Berlin: Springer)
Barnes, A. 1992, J. Geophys. Res., 97, 12,105
Dewar, R. L. 1970, Phys. Fluids, 13, 2710
Fisk, L. A. 2003, J. Geophys. Res., 108, 1157
Frazin, R. A., & Janzen, P. 2002, ApJ, 570, 408
Groth, C. P. T., DeZeeuw, D. L., Gombosi, T. I., & Powell, K. G. 2000, J. Geophys. Res., 105, 25053
Hammer, R. 1982, ApJ, 259, 767
Jacques, S. A. 1977, ApJ, 215, 942
McKenzie, J. F., Axford, W. I., & Banaszkiewicz, M. 1997, Geophys. Res. Lett., 24, 2877
Mikić, Z., Linker, J. A., Schnack, D. D., Lionello, R., & Tarditi, A. 1999, Phys. Plasmas, 6, 2217
Parker, E. N. 1963, Interplanetary Dynamical Processes (New York: Interscience)
Pneuman, G. W., & Kopp, R. A. 1971, Sol. Phys., 18, 258
Roussev, I. I., et al. 2003, ApJ, 595, L57
Suess, S. T., Wang, A.-H., Wu, S. T., Poletto, G., & McComas, D. J. 1999, J. Geophys. Res., 104, 4697
Suzuki, T. K. 2006, ApJ, 640, L75
Suzuki, T. K., & Inutsuka, S. 2005, ApJ, 632, L49
Tóth, G., et al. 2005, J. Geophys. Res., 110, A12226
Usmanov, A. V. 1993, Sol. Phys., 146, 377
Usmanov, A. V., & Goldstein, M. L. 2003, J. Geophys. Res., 108, 1354
Usmanov, A. V., Goldstein, M. L., Besser, B. P., & Fritzer, J. M. 2000, J. Geophys. Res., 105, 12675
Wang, Y.-M., & Sheeley, N. R. 1990, ApJ, 355, 726
Wu, S. T., Guo, W. P., Michels, D. J., & Burlaga, L. F. 1999, J. Geophys. Res., 104, 14789